Optical properties of Feedhorn-coupled TES polarimeters for CMB polarimetry

L.E. Bleem*, J.W. Appel†, J. E. Austermann**, J.A. Beall‡, D. T. Becker‡, B.A. Benson*, J.Britton‡, J.E. Carlstrom*, C. L. Chang*, H.M. Cho‡, A.T. Crites*, T. Essinger-Hileman†, W. Everett*, N.W. Halverson**, J.W. Henning**, G.C. Hilton‡, K.D. Irwin‡, J. McMahon*, J. Mehl*, S.S. Meyer*, M.D. Niemack‡, L.P. Parker†, S.M. Simon**, S. T. Staggs†, C. Visnjic†, K.W. Yoon‡ and Y. Zhao†

* *Kavli Institute for Cosmological Physics, University of Chicago, 5640 South Ellis Avenue, Chicago, IL 60637, USA*

† *Joseph Henry Laboratories of Physics, Jadwin Hall, Princeton University, Princeton, NJ, 08544, USA*

** *Center for Astrophysics and Space Astronomy, Department of Astrophysical and Planetary Sciences and Department of Physics, University of Colorado, Boulder, CO 80309, USA*

‡ *NIST Quantum Devices Group, 325 Broadway Mailcode 817.03, Boulder,CO, USA 80305, USA*

Abstract. We present data characterizing the optical properties of feedhorn-coupled TES polarimeters useful for future CMB measurements. In this detector architecture, TES bolometers are coupled to radiation through superconducting microstrip to a planar ortho-mode transducer inserted into waveguide. Filters in the microstrip define the pass bands for the detectors. We will present measurements of the co-polar optical efficiency, the cross-polar isolation and the detector bandpass and compare these results to expectations from simulations.

Keywords: cosmology, cmb, polarimeter
PACS: 95.75.Hi, 95.85.Bh, 98.80.Es

INTRODUCTION

Over the last three decades ever more exquisite measurements of the cosmic microwave background temperature anisotropies have been made. These experiments have placed stringent constraints on cosmology (see [1]). Recent experiments have probed the polarization spectrum. The "E-Mode" or curl free component of this polarization has been measured with high sensitivity. The "B-mode" (divergence free) signal is much fainter, and has not yet been detected. Measurement of the faint B-mode signal places limits on neutrino masses and provides insights into the energy scale of inflation [2]. While individual detectors have achieved nearly background limited sensitivities, in order to achieve the required sensitivity to probe the B-mode polarization it is necessary to expand to large arrays of detectors. In this work we present optical measurements of a prototype polarization pixel designed to be built in such an array.

PIXEL DESIGN

A fabricated pixel is shown in Figure 1. The beam of the pixel is defined by a corrugated feedhorn. The feedhorn couples radiation onto the pixel via the fins of a planar orthomode transducer (OMT) inserted into waveguide [3]. Leading out of the OMT there is an alternating coplanar waveguide and microstrip transforming section to better match the low impedence of the superconducting niobium microstrip to the high impedence OMT fins. The passband is defined by microstrip filters before the signal is terminated in lossy gold resistors and read out by a transition edge sensor (TES)[4].

FILTER DESIGN

Traditionally, observation bands have been defined using elements in the optical path of the instrument, such as wire mesh filters. Our pixel design allows another option: constructing the filters in microstrip for on-chip processing.

We chose a 5-pole Chebyshev $\lambda/4$-shorted stub filter as our bandpass filter. The desired -3 dB band edges were 127 & 164 GHz. Design formulas for these filters are available in standard references [5, 6]. The simple rectangular geometry makes these filters easy to fabricate and simulate using 2.5D EM simulators.

Five poles were chosen to give swift roll-off at the band edges. $\lambda/4$-stub filters have harmonic passbands at frequencies of 3, 5, 7, etc times the design frequency.

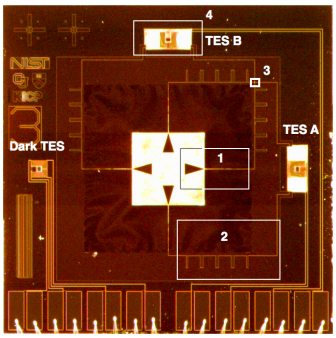

FIGURE 1. Photograph of prototype pixel. Boxed are: (1)Planar OMT fin to CPW-microstrip transistion, (2) microstrip bandpass and lowpass filters, (3) microstrip crossover, and (4)TES island with TES and lossy-gold absorbers. Also labeled are the two polarization channels, A and B as well as the dark channel that is not connected to the OMT. The dark channel is used for diagnostic purposes.

They are also susceptible to narrow spikes in transmission near 2, 4, and 6 times the design frequency if not tuned correctly [6]. To suppress these resonances we designed two simple stepped impedance low-pass filters with roll-offs at 190 and 310 GHz.

Simulation of the filter stack in Sonnet EM [7] showed that out-of-band leakage should be below -30 dB up to and past the Nb gap frequency of 740 GHz[8]. We compare these simulation results with the measured spectra in the next section.

MEASURED SPECTRUM

Spectra were obtained using a symmetric polarizing Michelson Fourier Transform Spectrometer (FTS)[9]. At one input port we have either a 1000C thermal blackbody or a 77K piece of eccosorb that we use as our source. A curved piece of light pipe placed at the corresponding output port runs up to the window of the dewar where the device is mounted. We have covered the offset pair of additional ports with 300K eccosorb to provide an isothermal reference and to help damp spurious reflections through the FTS. The FTS is calibrated in a frequency range between 45 and 3000 GHz and has a resolution of 2GHz. Scans were taken at a variety of speeds between .25 and 2 optical cm/s with sampling rates of either 128 or 512 Hz.

Inside the dewar, the device being tested is mounted in a brass holder that is screwed into a 350mK cold stage. The holder is connected to a corrugated feed horn via a two piece square to circular waveguide transformer. The waveguide cutoff of the holder is 115GHz , and does not define the pixel's lower band edge. The pixel is coupled to 300K via three separated pieces of lightpipe thermally

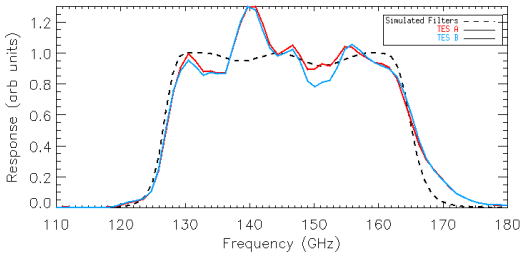

FIGURE 2. Measured Spectrum of a Prototype Pixel. Plotted are the simulated filter response function as well as the measured spectral response for polarization channels A and B. Note that the response for channels A and B were scaled so that the lower edge of the band roughly matched the simulated results.

sunk at 4K, 77K and 300K. At 4K we have capped the light pipe with 1/8" of fluorigold and 1/8" of expanded teflon to roll off high frequency radiation. At 77K a pair of 1/8" pieces of expanded teflon cover the light pipe on the 300K side. Finally there is a 15 mill polypropylene window to 300K. There are small misalignments/tilts at each light pipe juncture.

Figure 2 shows measured spectra from both polarization channels of a single test pixel as well as the simulated pass band of the microstrip filters. The measured spectra are plotted assuming a flat spectral source, (ie assuming that the source is single-moded and beam filling). However, as the light pipe setup limits the beam, some spectral dependence up to ν^2 is expected. We expect 25% ripples due to channel spectra from our plastic filters. We measure -3 dB band edges at 128GHz and 165GHz which compares favorably with the predictions from simulations (127GHz and 164GHz). However, the high frequency roll-off is a bit shallower than expected. While the band edges are well defined from scan to scan, we find that modifying the coupling optics between the dewar and the FTS changes the amplitude of the ripples in the band. Because of the difficulty of correctly normalizing the band in the presence of these ripples, the plotted spectra have been scaled so that the slope of the lower band edge roughly matches the simulated filter response.

One unexpected problem was the presence of large amounts of coupling outside of our desired band. This out of band power was confirmed with chopped thick grill measurements. As seen in Figure 3 this excess power does not display narrow resonances at the expected filter harmonics and extends well above the Nb bandgap frequency of 740GHz leading us to believe the power is not being coupled through the microstrip lines. In this spectra, the high-frequency leak is being sharply rolled off by the 1/8" fluorigold in our optics chain. Our primary candidate for this excess power is radiation coming down the waveguide leaking into a 50 μm air gap be-

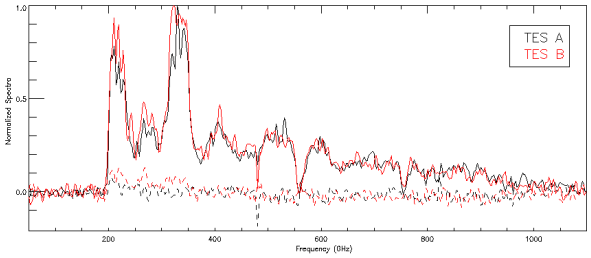

FIGURE 3. Spectra of prototype pixel through a 200GHz high pass filter. The spectra is normalized to the peak of the response. Plotted are the real (solid) and imaginary (dashed) portions of the FTS spectra. Taking the imaginary component as a measure of our noise, we see that the signal is wideband extending well beyond 740GHz, the niobium cutoff frequency. Structure in the spectra comes from the thick grill filter, atmospheric lines, roll off from our plastic high frequency attenuating filters, as well as structure of the high frequency leak itself.

tween the pixel and the bottom of the brass cover piece and then coupling directly onto the TES island (via the on-chip heater, the lossy gold terminations, or the TESs themselves). A pixel without the onboard heater has been fabricated to explore one of these hypotheses.

OPTICAL EFFICIENCY AND CROSS POLAR ISOLATION

The optical efficiency is measured with a polarized cold load. The cold load and test pixel are enclosed in a dip probe dewar. The cold load consists of a waveguide section filled with absorbing material with a conical space carved out in the middle to reduce reflection. This load is heated with a normal wire that is wrapped around it, and its temperature is measured with a diode that is located at the top end of the load. The cold load is mounted on a standard waveguide flange that connects to a 10 cm long WR6 stainless steel waveguide. This waveguide, which is heatsunk to 1K in the middle and at 0.3K at the opposite end from the cold load, is used to thermally isolate the cold load, which can be heated to 30 K, from the 0.3 K stage. The other end of the stainless steel waveguide is connected to a copper waveguide that completes a 90 degree turn to align itself with the input of the brass module where the detector is located. Between the rectangular output of the waveguide (which determines the polarization) and the square input of the module there are three shim pieces. One is an adiabatic transition between rectangular and circular waveguide, and the other two make up a circular to square transition. These shim pieces induce negligible cross-polarization signal .

We quantify the response of the detectors to changes in the cold load temperature (T_{CL}) by measuring the bias power (P_{tes}). At a constant bath temperature, P_{tes} plus the optical loading equals a constant. Therefore the difference in P_{tes} at two cold load temperatures is the same as the change in optical loading. This optical loading can also be predicted by considering the power a black body at T_{CL} emits in our frequency band onto a single mode detector. This number must be corrected for the stainless steel waveguide loss, and the extra power emitted by the hot section of the waveguide.

The power loading from the cold load P_{CL} may be expressed as:

$$P_{CL} = \int \int_{4\pi} A_e(\theta,\phi)\frac{B_\nu}{2} d\Omega d\nu, \tag{1}$$

where B_ν is the blackbody spectrum:

$$B_\nu = \frac{2h\nu^3}{c^2}\frac{1}{e^{\frac{h\nu}{kT}}-1}, \tag{2}$$

and $A_e(\theta,\phi)$ is the effective area of the detector. For a detector that perfectly couples to a single mode the effective area is just $\lambda^2/4\pi$. Therefore the maximum power loading from the cold load at a temperature T in the frequency band between ν_0 and ν_1 is:

$$P_{CL} = \int_{\nu_0}^{\nu_1} \frac{h\nu d\nu}{e^{\frac{h\nu}{kT}}-1}. \tag{3}$$

This loading estimate is corrected for a 51% loss across the 10 cm stainless steel waveguide. The loss across the waveguide was estimated by comparing measurements made with a 10cm and a 15cm stainless steel waveguide. To the cold load power we add the power emitted by the 5cm warm section of the waveguide that is located between the cold load and the 1K heat sink. The emissivity of this section is assumed to be 0.3, the same as the fractional power loss through it.

The predicted optical loading as a function of cold load temperature is given by the wide solid line in the left panel Figure 4. The measured optical power differences are plotted as the stars(cross-polar channel), crosses (co-polar channel) and circles ("dark" channel not connected to the microstrip). Notice that all of the channels see a power signal even though we only expect to see power in the polarization that is coupled to TESB. The majority of the power that couples to TESA and the dark bolometer is believed to come from radiation at frequencies higher than the band. At these higher frequencies the waveguide becomes multi-moded and radiation from both polarizations can propagate. As discussed in the FTS results, the mechanism through which this high frequency power couples to the detectors is not yet understood. In addition, because the waveguide losses and the filter roll off in the FTS measurement scale differently, it is difficult to directly compare the level of out of band power between these two measurements.

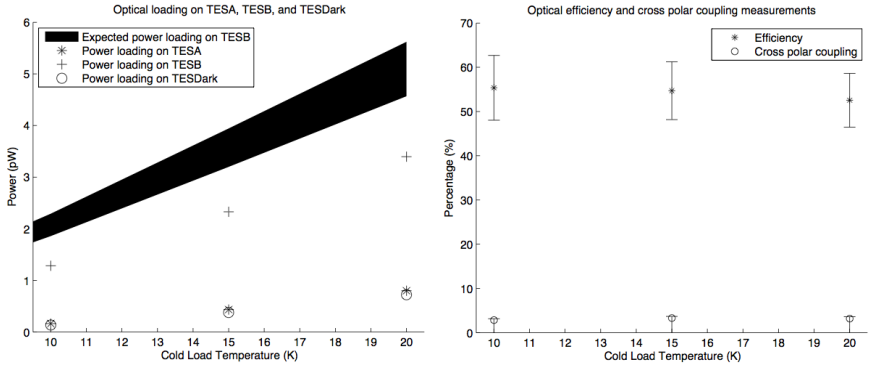

FIGURE 4. Optical Efficiency Measurements. In the left panel are the measured optical power differences from 2.5K for the cross polar channel, TES A (stars), the copolar channel, TES B(crosses), and the Dark TES (circles), which we take as a measure of the out of band power contribution. The statistical errors on the measurement are smaller than the size of the markers. Not included are the 5% uncertainty in the shunt resistance or the small uncertainties in the loading from the warm waveguide. The wide solid swatch shows the predicted optical loading with uncertainties. In the right panel are measured optical efficiency (stars) and crosspol coupling (circles) as a function of internal cold load temperature.

If we assume that the out of band power is distributed equally amongst the three channels, and that the dark TES can only see out of band radiation, the in-band power is equal to the power on TESB minus the power on the dark TES. Comparing this in-band power to the predicted optical loading from the cold load yields an optical efficiency of 54%. The right panel of Figure 4 shows the estimated optical efficiency (stars) taking into account IV measurement error, an uncertainty of 5% on the electrical conductivity of stainless steel, and a 3% uncertainty in the length of the waveguide. Not included are the 5% uncertainty in the shunt resistance or the small uncertainties in the loading from the warm waveguide. Using the same assumptions we can find the cross polar response by subtracting the power on the dark pixel from TES A. Plotted as circles are the upper limits on the cross-polar leakage from these measurements of 3%. See [3] for a discussion of the expected OMT cross-polarization properties.

CONCLUSION

We have prototyped a polarization sensitive pixel for use in future CMB Experiments. The device has co-polar coupling of 54% and cross-polar coupling of less than 3% across a band from 128-165GHz.

ACKNOWLEDGEMENTS

Work at the University of Chicago is supported by the National Science Foundation through grant ANT-0638937 and the NSF Physics Frontier Center grant PHY-0114422 to the Kavli Institute of Cosmological Physics at the University of Chicago. It also receives generous support from the Kavli Foundation and the Gordon and Betty Moore Foundation. The work at NIST is supported by the NIST Innovations in Measurement Science program. Work at the University of Colorado is supported by the National Science Foundation through grant AST-0705302. The work at Princeton University is supported by Princeton University and the National Science Foundation through grants PHY-0355328 and PHY-085587.

REFERENCES

1. E. Komatsu, et al., *ApJS*, 180, 330-376, 2009.
2. Baumann, et al. *Probing Inflation with CMB Polarization*, arXiv:0811.3919v1, 2008.
3. McMahon, J. et al. "Planar Orthomode Transducers for Feedhorn-coupled TES Polarimeters" , LTD 13 Poster 2009.
4. Irwin, K.D. *Appl. Phys. Lett. 66*, 1998 (1995); DOI:10.1063/1.113674
5. Hong J. S. and M. Lancaster. *Microstrip Filters for RF/Microwave Applications* John Wiley & Sons, New York, J. 2001.
6. Matthaei G., Young L., Jones. *E.M.T. Microwave Filters, Impedance-Matching Networks, and Coupling Structures* Artech House, Norwood, 1980.
7. Sonnet Suites, Sonnet Software Inc, 100 Elwood David Road, North Syracuse, NY 13212
8. Van Duzer, T. and Turner, C.W. *Principles of Superconductive Devices and Circuits*. Prentice-Hall, New York, 1999.
9. Shoemaker, D. H. *A Fourier Transform Spectrometer for Millimeter and Submillimeter Wavelengths*, Unpublished master's thesis. Massachusetts Institute of Technology, 1980.